nature communications

Article

https://doi.org/10.1038/s41467-025-56033-3

Diffusion-driven transient hydrogenation in metal superhydrides at extreme conditions

Received: 28 August 2024

Accepted: 7 January 2025

Published online: 29 January 2025

Check for updates

Yishan Zhou[1,8], Yunhua Fu[1,2,8], Meng Yang[1,8], Israel Osmond[3], Rajesh Jana[1], Takeshi Nakagawa[1], Owen Moulding[4], Jonathan Buhot[5], Sven Friedemann[5], Dominique Laniel[3] & Thomas Meier[6,7]

In recent years, metal hydride research has become one of the driving forces of the high-pressure community, as it is believed to hold the key to superconductivity close to ambient temperature. While numerous novel metal hydride compounds have been reported and extensively investigated for their superconducting properties, little attention has been focused on the atomic and electronic states of hydrogen, the main ingredient in these novel compounds. Here, we present combined ^{1}H- and ^{139}La-NMR data on lanthanum superhydrides, LaH_x, ($x = 10.2 - 11.1$), synthesized after laser heating at pressures above 160 GPa. Strikingly, we found hydrogen to be in a highly diffusive state at room temperature, with diffusion coefficients in the order of $10^{-6} cm^2 s^{-1}$. We found that this diffusive state of hydrogen results in a dynamic de-hydrogenation of the sample over the course of several weeks, approaching a composition similar to its precursor materials. Quantitative measurements demonstrate that the synthesized superhydrides continuously decompose over time. Transport measurements underline this conclusion as superconducting critical temperatures were found to decrease significantly over time as well. This observation sheds new light on formerly unanswered questions on the long-term stability of metal superhydrides.

The pursuit of room-temperature superconductivity has driven significant advancements in high-pressure physics, with metal hydrides emerging as prime candidates for achieving this elusive goal[1]. Theoretical predictions have played a crucial role in guiding experimental efforts, suggesting that hydrogen-rich compounds could exhibit superconductivity at temperatures near or even above ambient condition when subjected to extreme pressures[2,3]. In particular, first-principles density functional theory (DFT) calculations predicted the formation of novel metal hydrides with complex structures and extraordinary superconducting properties[4]. These results have sparked intense research activity, leading to the synthesis of a variety of metal hydrides, including those based on sulfur[5], yttrium[6], and lanthanum[7], which have demonstrated superconductivity close to ambient temperatures at high pressures. Among these, lanthanum superhydrides have garnered considerable attention following experimental reports of superconductivity at temperatures exceeding 250 K at pressures of around 170 GPa. Such discoveries are rooted in the idea that under sufficient pressure, hydrogen atoms in these compounds adopt an arrangement facilitating Cooper pair formation[8]. Both theoretical models and the observation of the isotope effect in these systems suggest that the observed superconductivity originates from strong electron-phonon coupling, in which the hydrogen atoms

[1]Center for High-Pressure Science and Technology Advance Research, Beijing, China. [2]School of Earth and Space Sciences, Peking University, Beijing, China. [3]Center for Science at Extreme Conditions, Edinburgh, UK. [4]Institut Néel CNRS/UGA UPR2940, 25 Avenue des Martyrs, 38042 Grenoble, France. [5]H.H. Wills Physics Laboratory, University of Bristol, Bristol, UK. [6]Shanghai Key Laboratory MFree, Institute for Shanghai Advanced Research in Physical Sciences, Shanghai 201203, China. [7]Shanghai Advanced Research in Physical Sciences (SHARPS), Shanghai 201203, China. [8]These authors contributed equally: Yishan Zhou, Yunhua Fu, Meng Yang. e-mail: thomasmeier@sharps.ac.cn

provide significant electronic density of states at the Fermi energy and high-frequency phonon modes[9].

However, despite these experimental and theoretical advances, significant gaps remain in our understanding of the atomic and electronic behavior of hydrogen within these dense metal hydrides. Hydrogen, due to its single electron, small interaction cross sections and high mobility, poses substantial challenges for standard high pressure experimental characterization methods. While theoretical calculations provide valuable insights into possible hydrogen configurations and the electronic structures of such materials, direct experimental probing of hydrogen's role has been limited–despite being of the utmost importance.

Owing to its exceptional sensitivity to hydrogen nuclei by sensing minuscule local magnetic fields in condensed matter systems, nuclear magnetic resonance (NMR) spectroscopy has proved to be an ideal tool for investigating structural, electronic and dynamic properties of metal superhydride systems. Recent advances in the field of in-situ high-pressure NMR led to a significant improvement of resonator sensitivities[10,11], pressure stability[12,13] and spectral resolutions[14,15], allowing for routine experimentation well into the mega-bar regime[16–18]. Pioneering experiments on iron and copper hydride systems found a significant enhancement of the hydrogen Knight shift[19] upon compression, indicating an increasing electronic density of states via the formation of a conductive sublattice of hydrogen atoms[20]. Furthermore, it could be shown that hydrogen atoms exhibit self-diffusion coefficients in the order of $10^{-8} cm^2 s^{-1}$, even at elevated pressures but room temperature[21]. Finally, developments in the field of quantitative high-pressure NMR spectroscopy[22] led to a direct and stand-alone quantification method of hydrogen atoms' concentrations in hydrides[23].

In this context, we present an investigation addressing the aforementioned experimental and theoretical gaps by employing NMR spectroscopy to probe the atomic and electronic states of hydrogen in lanthanum superhydrides (LaH_x (x = 10.2–11.1)) synthesized above 160 GPa. This study utilizes a combination of ^1H- and ^{139}La-NMR which reveals the highly diffusive nature of hydrogen within these compounds, which leads to a gradual de-hydrogenation of the synthesized samples over time, inferred to strongly affect the stability and superconducting properties of the synthesized superhydrides.

Results and discussion

For NMR experiments, four panoramic non-magnetic diamond anvil cells (DACs) have been prepared with diamond anvils having culets of 100 μm in diameter. Further details are provided in the Methods section. All cells were loaded with lanthanum trihydride, LaH_3 and ammonia borane, NH_3BH_3, acting as a pressure transmitting medium as well as a hydrogen source. Samples were prepared by mixing LaH_3 and NH_3BH_3 powders with a stoichiometric ratio of about 1:4. Synthesis of lanthanum superhydrides was achieved by laser heating the four DACs above about 1500 K employing a double-sided laser heating arrangement similar to previous work[20,21]. All NMR measurements were conducted at room temperature.

Figure 1 shows recorded spectra of the ^{139}La- and ^1H-spin subsystem before and after laser heating at 170 GPa. Before laser-heating (blue spectra in Fig. 1), the lanthanum signal of LaH_3 exhibits a single sharp resonance of about 8 kHz in line-width. Given that ^{139}La is a $I = 7/2$ quadrupolar spin system with nuclear quadrupole moments of about $20 fm^2$ [24], making it very sensitive to local structural distortion leading to line-widths >100 kHz, we conclude the precursor material to be in an almost perfect cubic environment leading to vanishing quadrupolar spin interactions[25] at the La lattice sites. This observation is in accordance with X-ray diffraction data[26]. The hydrogen signal of LaH_3 was found to be broadened to about 50 kHz line-width, caused by direct homo-nuclear dipole-dipole interactions between adjacent hydrogen atoms[27]. Microscale quantitative NMR (μQ-NMR) measurements, comparing the time-domain signal-to-noise ratios in both the ^{139}La and

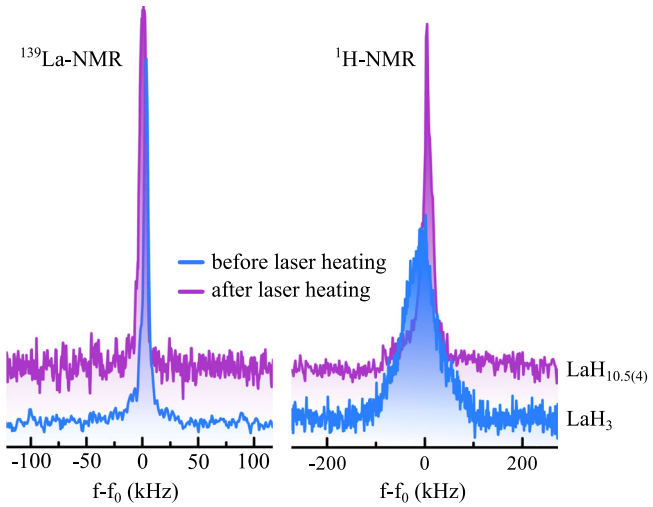

Fig. 1 | Lanthanum and hydrogen signals before and after laser heating above approximately 1500 K at 170 GPa. Left Sharp resonances of both LaH_3 and $LaH_{10.5(4)}$ indicate the absence of significant electric field gradients at the La-sites, in agreement with diffraction methods and ab-initio DFT calculations[26,28]. Right While the ^1H-NMR resonances of the hydrogen spin sub-system in LaH_3 are predominantly broadened by direct homo-nuclear dipole couplings, we found the corresponding resonances after laser heating to be significantly sharper, indicating enhanced hydrogen mobility[33]. Carrier frequencies f_0 were 55.95 MHz and 395 MHz for ^{139}La and ^1H respectively. For more information, see methods section. Spectra taken prior to laser heating are in blue, after laser heating in purple.

^1H channels[22,23], found a hydrogen-to-lanthanum ratio of $H/La = 3.1(2)$, in very good agreement with the anticipated stoichiometry for lanthanum trihydride. Frequency shifts for both spin sub-systems were determined to be ~2800Hz/MHz (or ppm) and ~ 10Hz/MHz for ^{139}La and ^1H, respectively.

The purple spectra in Fig. 1 show recorded data after laser heating. μQ-NMR measurements revealed a H/La of 10.5(4) in this particular cell. Presumably due to slightly different synthesis pressures (i.e. from 168 to 176 GPa) as well as laser-heating temperatures, hydrogen contents in all other cells varied from 10.2(3) to 11.1(4). The rather sharp line-widths of the quadrupolar ^{139}La spin system indicates vanishing quadrupolar interactions, indicating a cubic or almost cubic local environment of lanthanum atoms in LaH_{10+x}, in good agreement with recent ab-initio DFT calculations by Chen et al.[28]. However, since no diffraction experiments have been done in those cells, we cannot rule out long-range distortions from cubic symmetry which has been observed in heterogeneous lanthanum hydride samples under similar pressures[29].

Recorded hydrogen spectra of $LaH_{10.5(4)}$ at 170 GPa exhibit strikingly sharp resonances of ≈1.35kHz FWHM. Given that DFT-calculated average hydrogen-hydrogen distances in a compound with a face centered cubic fcc, space group $Fm\bar{3}m$) arrangement of lanthanum with $H/La \approx 10$ are in the order of ~ 1.0–1.1 Å[30], we would expect Pake-like[31] resonance line-widths in the order of 90–120 kHz. Such significantly sharpened line-widths as observed here are often associated with high degrees of mobility such as in gases or liquids[32,33].

To elucidate the possibility of enhanced mobility of hydrogen atoms in this lanthanum superhydride, we recorded several spin echo trains with increasing de-phasing times[34]. Figure 2 shows recorded hydrogen spin echoes at 170 GPa. As it can be seen, echoes are observable at delay times of up to 1 ms and beyond. In general, the transverse relaxation (T_2) in condensed matter solid-state systems tends to become shorter under pressure, e.g., on the order of 20 − 50μs, whereas our experiments indicate a spin-spin relaxation of $T_2 = 1.5(2) ms$. Additionally, we conducted saturation recovery experiments in order to determine the longitudinal spin-lattice relaxation time (T_1) of the hydrogen spin sub-system, see Fig. 3. Strikingly we

https://doi.org/10.1038/s41467-025-56033-3

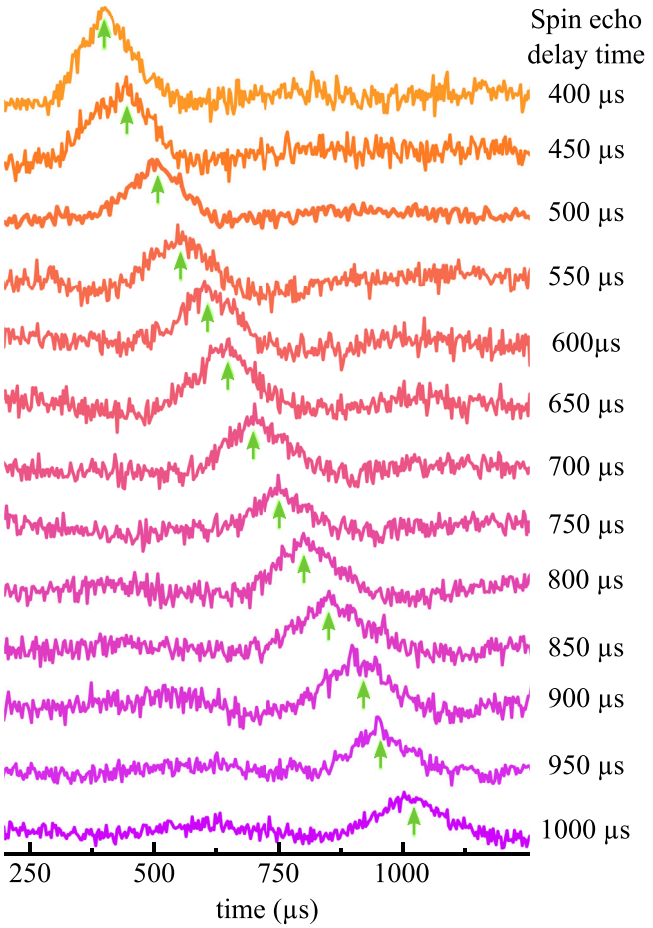

Fig. 2 | ^1H-NMR time domain response after spin echo excitation in $LaH_{10.5(4)}$ at 170 GPa and room temperature. Hydrogen spin echoes could be refocused at large delay times of up to 1 ms, indicative of greatly enhanced longitudinal spin relaxation times T_2. Green arrows indicate echo centers. All time domain responses were offset for better comparison.

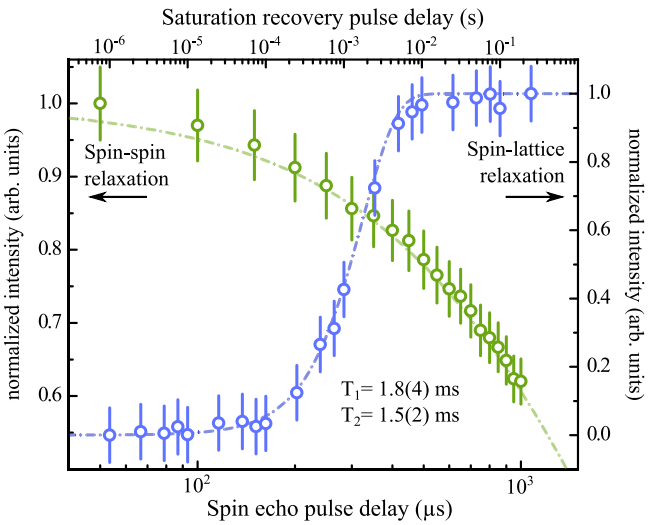

Fig. 3 | Comparison between spin-lattice (T_1 and spin-spin T_2) relaxation times at 170 GPa at room temperature. Both saturation recovery experiments and delayed spin echoes suggest that $T_1 \approx T_2$, implying that motional correlation times of hydrogen atoms in lanthanum superhydrides approach spectral time scales (see text), evidencing the highly diffusive state of hydrogen atoms in this system. Lines are respective fits for transverse and longitudinal relaxation times assuming single exponential decays. Error bars were determined from intensity calculations and amount to up to 5% at each spectrum.

found that both T_1 and T_2 are almost identical, evidencing that correlation times of atomic motion of the hydrogen atoms to be much faster than spectral time scales $1/\omega_0 = 1/(2\pi f) \approx 0.4ns$. In this so-called extreme narrowing limit ($\omega_0\tau_c \ll 1$) both relaxation times converge, leading to an effective cancellation of broadening spin interactions like homo-nuclear dipole-dipole interaction[35–37].

Contribution to T_1 via hyperfine interactions between conduction electrons and hydrogen nuclei as described by Korringa[38] can be considered low as the observed hydrogen Knight shift in LaH_{10+x} remains very low, in the range of 20 Hz/MHz. Therefore diffusional motion of hydrogen atoms within Lanthanum superhydride most likely dominates spin relaxation processes.

Indeed, in the limit of extreme narrowing, correlation times of motion -and thus atomic diffusion coefficients- become directly proportional to the transverse spin-lattice relaxation time via[21,37]:

$$D = \frac{3\pi}{10} \cdot \frac{\gamma_n^4 \mu_0^2 h^2 N_0 T_1}{a} \quad (1)$$

with $\gamma_n = 26.752 \cdot 10^7 radT^{-1}s^{-1}$ the gyromagnetic ratio of hydrogen atoms, N_0 the atomic number density, a the shortest contact between two hydrogen atoms and $h = 6.626 \cdot 10^{-34}Js$ the Planks constant. Provided a unit cell volume of about 143 $Å^3$ [29] for LaH_{10+x}, an atomic number density for hydrogen atoms of about $N_0 \sim 10^{23}cm^{-3}$ can be assumed with shortest H-H distances on the order of 1 Å. Thus, the diffusion coefficient of hydrogen atoms in LaH_{10+x} can be estimated to be in the order of $D \sim 10^{-6}cm^2s^{-1}$.

Recent ab-initio calculations by Caussé et al.[39] predict similar diffusion coefficients in lanthanum superhydrides, albeit at higher temperatures. We speculate that the strong quantum fluctuations relevant for the stability of LaH_{10}[30] give rise to the large diffusion coefficient for hydrogen at room temperature.

Experiments at ambient conditions suggested that highly diffusive hydrogen in metal hydrides might play a significant role in their observed decomposition over longer time periods[40,41]. Indeed, diffusion-driven hydrogen desorption is a commonly known effect in hydrogen storage materials and low-H content hydrides at ambient conditions[42,43].

In order to examine the effect of hydrogen desorption, we measured both ^{139}La- and ^1H-NMR signals of all prepared four diamond anvil cells over a time period of 50 to 70 days without otherwise changing experimental conditions. Pressures were checked on a daily basis, without any significant changes -within 15 GPa- over the investigated time periods. Figure 4 shows the recorded lanthanum and hydrogen signals in the sample cavity.

Directly after the synthesis of the high hydrogen content compounds through laser-heating, the dominant ^{139}La signal was found at Knight shifts of about 900 Hz/MHz relative to an aqueous solution of $LaCl_3$, Fig. 4a. We observed an increase in the FWHM line-width to about 38 kHz, indicating slightly distorted local lanthanum environments and an onset of first order quadrupole interaction. However, no quadrupolar satellite signals of higher-order quantum transitions could be observed, indicating the lanthanum sites remain in isotropically cubic local environments. Remarkably, over time, the lanthanum NMR signals were found to gradually shift down-field (towards higher shift values), whereas overall signal intensities -and thus the number of lanthanum atoms in the sample cavity- remained unchanged. About 50 days after the initial sample synthesis, we found the ^{139}La-NMR signal to be shifted to 2950 Hz/MHz, which is only about 150 Hz/MHz higher than the observed Knight shift of the LaH_3 precursor material.

At the same time, we observe a gradual loss of signal intensity in the ^1H-NMR spectrum associated with the synthesized LaH_{10+x} samples, as shown in Fig. 4b. No significant resonance shift could be observed. Recorded spectra suggest an increase of FWHM line-widths as time progresses. Furthermore, the formation of a broad signal of

https://doi.org/10.1038/s41467-025-56033-3

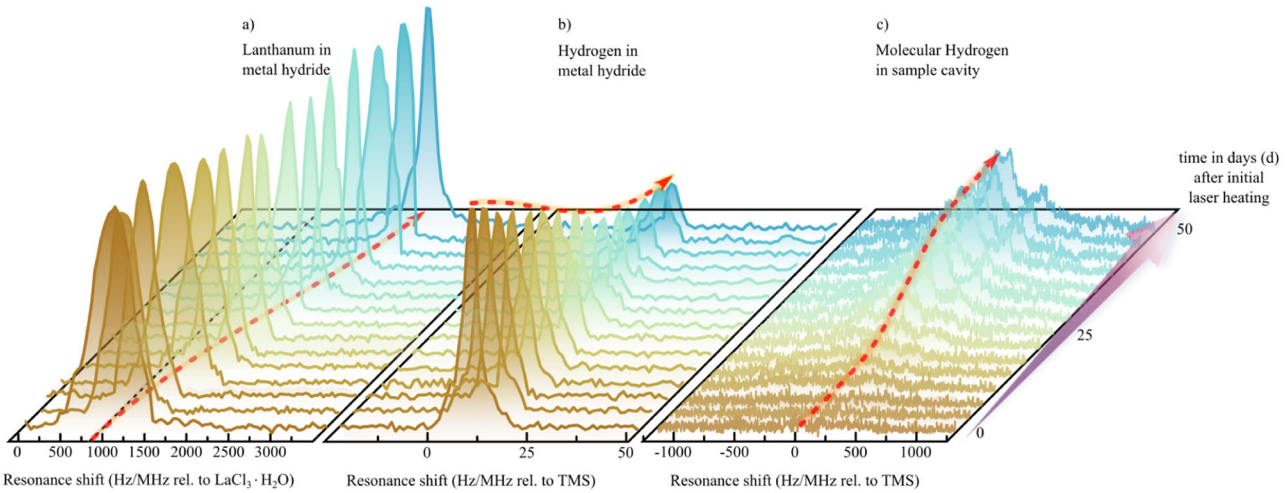

Fig. 4 | Long-term evolution of NMR spectra in days after initial laser heating at 170 GPa. a ^{139}La-NMR spectra remain almost constant intensities while resonance frequencies gradually shift towards higher Hz/MHz values. **b** A progressive decrease in signal-intensity of the ^{1}H-NMR spectra of the metal hydride spin subsystem was observed while a simultaneous increase of molecular hydrogen in the sample cavity (**c**) was observed. Red lines are a guide to the eye. Carrier frequencies f_0 are identical to Fig. 1. Lanthanum and hydrogen shifts were referenced to an aqueous solution of Lanthanum chloride and Tetramethylsilane (TMS). Supplementary Figs. S4–S9 show similar data for all other experimental runs.

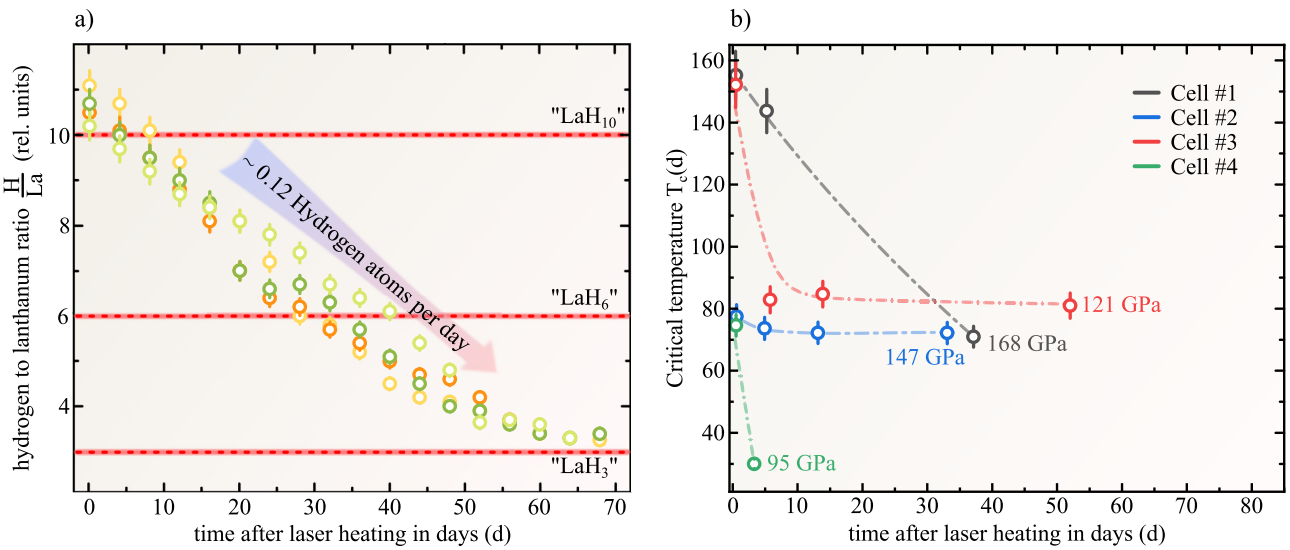

Fig. 5 | Long-term evolution of hydrogen contents in metal hydride compound and superconducting critical temperatures. a Evolution of the hydrogen-to-lanthanum ratio $\frac{H}{La}$ over the course of 68 days summarizing data of all four employed DACs at room temperature. $\frac{H}{La}$ was found to continuously decrease with time, asymptotically approaching the hydrogenation of precursor LaH_3, with a desorption-rate of about 0.12 hydrogen atoms per day. Error bars were determined via gaussian error propagation in the calculation of the $\frac{H}{La}$ ratios. **b** Evolution of the normalised superconducting critical temperature T_c after initial laser heating. Four DACs were laser heated at different pressures ranging from 95 to 168 GPa. As can be seen, all synthesised compounds express a significant decrease of T_c over time. Error bars were determined from transition width in the resistivity measurements (see Supplementary Fig. S10). Cells are numbered according to Supplementary Fig. S10.

about ~10^3 Hz/MHz was observed, as shown in Fig. 4c. This gradually appearing signal has striking similarities with recently observed ^{1}H-NMR signals of molecular hydrogen phase III[18] after the collapse of the spin isomer distinction which have been observed earlier[16].

The observation of a decrease in intensity of the ^{1}H-NMR signal associated with the synthesized lanthanum hydride, and the concurrent formation of molecular hydrogen in the sample cavity, indicates that hydrogen continuously desorbs out of the LaH_{10+x} across the pressure range studied. In order to illustrate this hypothesis, we conducted μQ-NMR experiments for each data collection. Figure 5a shows the resulting H/La ratios over the entire experimental observation period.

As can be seen, directly after laser heating, H/La ratios were found to be between 10.2(3) and 11.1(3) for synthesis pressures ranging from 168 to 176 GPa, close to previously reported hydrogenations in lanthanum superhydrides[7,29,44]. A continuous decrease in overall H/La atomic ratios in the metal hydride systems was found, with an average hydrogen loss of 0.12(5) atoms per day.

The horizontal red lines in Fig. 5a indicate H/La ratios associated with lanthanum hydride stoichiometries of LaH_x(x = 10, 6, 3). It was found that after about 30 days after initial laser heating, the overall hydrogen to lanthanum ratio decreased by almost 40%, indicating a gradual continuous transition from stoichiometries associated with LaH_{10} to LaH_6.

At observation periods longer than 50 days, data suggests a somewhat flattened out convergence to atomic ratios reminiscent of the lanthanum trihydride precursor. As this convergence remains

poorly resolved in the given data (Fig. 5a), observations at longer time intervals would be more indicative of whether a complete decomposition to the precursor materials is taking place. Unfortunately, measurements at longer times were not possible due to diamond failure caused by hydrogen diffusion and consequent embrittlement. However, hydrogen absorption and desorption studies on magnesium dihydride suggest that dynamic dehydrogenation over time converges to slightly higher H-contents than that of the precursor[45].

At this point it should be noted that due to diffusion of molecular hydrogen into the anvils and rhenium gaskets the desorption of hydrogen from the hydride and the increase in intensity of molecular hydrogen in the sample cavity, the relation between Fig. 4b, c, is only of qualitative nature rather than a quantitative observation. Furthermore, due to the broad resonance lines of molecular hydrogen, effective spin excitation—which is mandatory for any quantitative assessment-becomes difficult, effectively prohibiting a quantitative correlation to hydrogen desorption from the hydride systems.

For a clathrate hydride system in which high hydrogen content is expected to be beneficial for superconductivity, a decrease in the hydrogen content should result in a significant reduction of superconducting critical temperature as a function of time.

To elucidate this possibility, four new DACs have been prepared for transport measurements using lanthanum metal films and ammonia-borane[46–48]. It should be noted that due to different initial experimental conditions in those cells, synthesised hydrides were likely of lower hydrogen contents than the LaH_{10+x} compounds of the NMR studies and thus show lower initial superconducting transition temperatures than what would expect for hydrogenation values of $x \geq 10$. For more details, see Methods Section.

Figure 5b shows the experimental runs determining T_c, obtained over a time of up to 80 days. Laser heating produces T_c values up to 160 K observed immediately after laser heating. While the structure and stoichiometry of such initially synthesized hydride phases are unknown, T_c was found to drop sharply in the days following laser heating, before converging to significantly lower values between 70 and 85 K, well below that expected for $Fm\bar{3}m$ LaH_{10} of > 240K within this pressure range[7].

Given the here presented data, the following picture emerges. Directly after laser heating, lanthanum atoms occupy lattice sites resulting in vanishing electric-field gradients, in accordance with DFT structural search algorithms and diffraction experiments[7,29,44]. Our NMR data clearly shows the hydrogen atoms to be in a state of high atomic mobility, with diffusion coefficients in the order of $10^{-6} cm^2 s^{-1}$, several orders of magnitude more mobile than in known hydrides at ambient conditions[49,50]. This diffusive state of hydrogen leads, over time, to a dynamic desorption of hydrogen out of the synthesized hydrides, accompanied by a continuous release of molecular hydrogen phase III in the sample cavity. Using quantitative NMR methods, it could be shown that over the course of about 70 days, initially synthesized LaH_{10-11} samples approached a state reminiscent of almost full decomposition back to the precursor materials. Likewise, for the transport cell with the highest synthesis pressure (168 GPa), we observe a timescale for the decrease and stabilization of T_c comparable with the desorption timescale observed in NMR experiments at a similar synthesis pressure. Given differing sample geometries between NMR and transport experiments, a quantitative comparison of hydrogen diffusivities is however difficult and likely also depends on the relative amounts of excess molecular H_2 produced from the decomposition of NH_3BH_3, the amount of synthesized LaH_x and the hydrogen porosity of the gasket material itself.

At this point it should be noted that NMR measurements in diamond anvil cells often require different and somewhat simpler sample geometries than usual experimental setups used for transport experiments. Whereas transport measurements often require a more stringent sample geometry in order to fully bridge electrical contacts, NMR measurements are somewhat more flexible. Loading the sample cavity using finely ground powder of about $> 1\mu m$ grain sizes is preferable to ensure proper powder averaging of orientation dependent spin interactions like homo-nuclear dipole-dipole couplings or quadrupolar interactions[51].

Such fine dispersed powders are much more effectively hydrogenated upon the release of H_2 from NH_3BH_3 to form LaH_{10}, whilst the observed initial T_c in transport evidences only partial hydrogenation. The observation of a full superconducting transition is sensitive only to a continuous superconducting path between the electrical contacts, of which the highest T_c superconducting transition will dominate the observed resistance behavior. From the above transport data, we conclude that high-T_c lanthanum hydride phases with T_c values above 140 K are not stable for our presented measurements.

Furthermore, it needs to be mentioned that NMR probes the entire sample cavity in order to pick up faint nuclear induction signals after radio-frequency excitation. Thus, provided that this method relies greatly on the number of active NMR nuclei (nuclear spin $I > 0$), small grains of different stoichiometries might be below our detection limits. This is likely also the reason why observed NMR spectra, e.g., Figs. 1, 4, only show single signals, despite commonly accepted structural heterogeneity in DAC sample cavities after laser heating[29]. During sample synthesis, this heterogeneity has been tried to mitigate by de-focusing of laser spots, long-term exposure, as well as careful rastering over the entire sample cavity. Nevertheless, we cannot rule out the existence of different hydride systems in the sample cavities after laser heating, but given that all μQ-NMR analyses indicated atomic ratios of H/La > 10 we assume that LaH_{10+x} is the most dominant hydride phase synthesized.

The here observed phenomenon has significant implications for studies of hydride materials at high pressures. The desorption from higher hydrides like LaH_{10} is likely driven by the lack of a sufficient hydrogen reservoir in our experiments and most likely effects other experimental approaches. The absence of excess hydrogen is apparent in our experiments from the absence of an NMR signal of molecular hydrogen immediately after the synthesis of the NMR samples and the absence of a H_2 vibron in Raman measurements of our electrical transport samples. The desorption of hydrogen from the samples suggests that the chemical equilibrium with fully hydrogenated LaH_{10} may only be stable in the presence of excess hydrogen. This aspect should be taken into account to design future studies of hydrides at high pressures. It will also be interesting to check if the desorption can be halted at low temperatures as suggested by recent transport studies on La_4H_{23}[46]. We note that the desorption and the chemical instability might explain the large sample dependencies observed for higher lanthanum hydrides[7,52] and might similarly apply to yttrium hydrides[53]. By contrast, sulfur hydride (H_3S) samples show a stable T_c over years and lack large sample dependencies[1,48]. Understanding the differences in hydrogen diffusion and desorption in hydrides might pave a way to stabilise hydrides at lower and ambient pressure.

In summary, this work represents a novel viewpoint on metal hydrides under extreme conditions. It could be shown that the highly diffusive state of hydrogen atoms leads to transient hydrogen contents with highest values of H/La as well as highest values of T_c occurring in a narrow time frame directly after sample synthesis followed by steep declines in both quantities. This observation sheds new light on ongoing experimental controversies and opens up new questions on the theoretical treatment of potentially superconducting metal hydrides synthesised in diamond anvil cells.

Methods

NMR-DAC preparation

First, rhenium gaskets were indented to the desired thickness, usually $\lesssim 20$ µm. Sample cavities were drilled using specialized laser drilling equipment. After gasket preparation, the diamond anvils were covered

with a layer of 1 µm of copper or gold using chemical vapor deposition. To ensure electrical insulation of the conductive layers from the rhenium gasket, the latter were coated by a thin layer (≈500 nm) of Al_2O_3 using physical vapor deposition. The Lenz lens resonators were shaped from the conductive layer on the diamonds by using focused ion beam milling.

Before the final cell assembly, radio frequency resonators were prepared accordingly to their desired operation frequency. Pairs of high inductance solenoid coils (≈100 nH) for ^{139}La and ^{1}H-NMR frequencies at high fields were used as driving coil arrangements for the Lenz lens resonators' structure and were placed around each diamond anvil. After sample loading and initial pressurisation, the driving coils were connected to form a Helmholtz coil-like arrangement.

Pressure was determined using the shift of the first derivative of the first order Raman signal of the diamond edge, collected in the center of the anvils' culet. All DACs were fixed and connected to home built NMR probes equipped with customized cylindrical trimmer capacitors (dynamic range of ≈ 20 pF) for frequency tuning to the desired resonance frequencies and impedance matching to the spectrometer electronics (50Ω).

Proton and lanthanum shift referencing were conducted using the ^{63}Cu resonances of the Lenz lenses themselves as internal references taking into account the additional shielding of B_0 inherent to every DAC. These resonances were cross referenced with standard metallic copper samples at ambient conditions without a DAC. The resulting shift between both ^{63}Cu-NMR signals are then used as a primer for the NMR signals of the samples under investigation. Additionally, two DACs were prepared in the same way as described above and loaded with an aqueous solution of $LaCl_3$ for lanthanum referencing and with tetramethylsilane for hydrogen shift referencing. Both methods yielded similar results, with shifts varying by less than 5 ppm.

After pressurization to pressures above 160 GPa, double-sided laser heating to temperatures above 1200 K was achieved. In order to ensure a roughly homogeneous sample environment, laser heating was performed with defocused laser spots and the sample rastered several times. Resulting NMR signals did not show more than single signals above the detection limit.

NMR experiments

All NMR experiments were conducted on a modified 395 MHz proton frequency magnet, equivalent to a magnetic field of 9.28 T, using fully homemade NMR probes. ^{1}H-NMR spectra of lanthanum hydrides were recorded using single pulses with Gaussian shape modulation, with 14 µs pulse lengths at 800 mW power, 5 µs dead times and 10.000 accumulations. The spin echoes shown in Fig. 2 were recorded using a 16-phase cycle Hahn echo of Gaussian amplitude modulation with 14 and 28 µs pulse lengths, 800 mW pulse power and 40.000 accumulations. Solid echo spectra of molecular hydrogen phase 3 were recorded using a standard 8 phase cycle sequence with Gaussian pulse modulation with 6 µs pulse lengths, 20 µs pulse delays at 5 W power (40.000 accumulations). The lanthanum signals were acquired using a 8 phase cycle solid echo sequence of 4 µs pulses at 500 mW pulse power and 25 µs pulse delays (25.000 accumulations). All repetition times were chosen to optimise data acquisition times ($\approx 5 \cdot T_1$). All lanthanum spectra were recorded using solid echo pulse sequences with Gaussian modulation. Atomic ratios of H/La were determined using the method of time-domain quantification similar to Fu et al. [22].

The ^{1}H-NMR spin lattice relaxation time of the hydrogen reservoir, NH_3BH_3, was determined to be around 180s. Hydrogen signals depicted in this work were all recorded at significantly shorter repetition times of 10ms, thus any spurious hydrogen signals from the reservoir are effectively filtered out and are not observable in our experiments.

In the same vein, simultaneous detection of both hydrogen spin systems in the hydride and molecular hydrogen was mitigated provided that the repetition times for the hydride spin system was found much shorter than that of molecular hydrogen (about 1s). No signals of the hydride spin system was observed in the solid echo experiments employed to detect the uptake of molecular hydrogen.

A scan over a wide frequency range at ^{139}La-NMR frequencies have been conducted to ensure absence of satellites from the I = 7/2 lanthanum spin system. Furthermore all nutation experiments indicate a full degeneracy of all seven nuclear spin transitions of ^{139}La.

Time-domain quantifications, for H/La ratios calculation, have been determined using scan-normalized signal-to-noise ratios, i.e. $SNR/\sqrt{N_{scans}}$. With N_{scans} the number of accumulations for each experiment.

Transport cell preparation

Electrical transport measurements were carried out using diamond anvil cells equipped with diamonds with 50 μm culet. Gaskets were made from T301 stainless steel, preindented to a thickness below 40 µm. The center of the steel was then drilled out and replaced with a mixture of cubic-boron nitride and epoxy mixture to insulate electrodes from the gasket. Electrodes were formed by thin-film deposition of six tungsten and gold bilayers, followed by the deposition of metallic lanthanum (20 × 20 × 0.2 µm) directly onto the electrodes at the center of the culet.

Cells were closed with NH_3BH_3, employed as both the pressure-transmitting medium and the hydrogen source. After pressurization to a given target pressure, these cells were laser heated to 1200 K using a 1070 nm YAG laser with multiple 300 ms pulses. After heating, resistance measurements as a function of temperature were immediately performed, and then periodically over subsequent days to weeks using an AC-resistance bridge (SIM921, Stanford Research Systems) with a 100 μA excitation current.

Data availability

The NMR data supporting the findings of this study are available in the supplemental material. Transport measurement data generated in this study have been deposited in the University of Bristol database under https://doi.org/10.5523/bris.rajs1bybhrah2nf5py0llsm12. Source data are provided with this paper.

References

1. Drozdov, A. P., Eremets, M. I., Troyan, I. A., Ksenofontov, V. & Shylin, S. I. Conventional superconductivity at 203 kelvin at high pressures in the sulfur hydride system. *Nature* **525**, 73–76 (2015).
2. Ashcroft, N. W. Hydrogen dominant metallic alloys: High temperature superconductors? *Phys. Rev. Lett.* **92**, 1–4 (2004).
3. Zurek, E., Hoffmann, R., Ashcroft, N. W., Oganov, A. R. & Lyakhov, A. O. A little bit of lithium does a lot for hydrogen. *Proc. Natl Acad. Sci.* **106**, 17640–17643 (2009).
4. Pickard, C. J., Errea, I. & Eremets, M. I. Superconducting hydrides under pressure. *Annu. Rev. Condens. Matter Phys.* **11**, 031218–013413 (2020).
5. Nakao, H. et al. Superconductivity of pure H 3 S synthesized from elemental sulfur and hydrogen. *J. Phys. Soc. Jpn.* **88**, 123701 (2019).
6. Kong, P. et al. Superconductivity up to 243 K in the yttrium-hydrogen system under high pressure. *Nat. Commun.* **12**, 5075 (2021a).
7. Drozdov, A. P. et al. Superconductivity at 250 K in lanthanum hydride under high pressures. *Nature* **569**, 528–531 (2019).
8. Ashcroft, N. W. Metallic hydrogen: A high-temperature superconductor? *Phys. Rev. Lett.* **21**, 1748–1749 (1968).
9. Struzhkin, V. et al. Superconductivity in La and Y hydrides: Remaining questions to experiment and theory. *Matter Radiat. Extremes* **5**, 028201 (2020).
10. Meier, T. et al. Magnetic flux tailoring through Lenz lenses for ultrasmall samples: A new pathway to high-pressure nuclear magnetic resonance. *Sci. Adv.* **3**, eaao5242 (2017).

11. Meier, T. At Its Extremes: NMR at Giga-Pascal Pressures. In Graham Webb, editor, *Annual Reports on NMR Spectroscopy*, chapter 1, 1–74. Elsevier, London, 93 edition, (2018).
12. Meier, T. et al. NMR at pressures up to 90 GPa. *J. Magn. Reson.* **292**, 44–47 (2018).
13. Meier, T. Journey to the centre of the Earth: Jules Vernes' dream in the laboratory from an NMR perspective. *Prog. Nucl. Magn. Reson. Spectrosc.* **106–107**, 26–36 (2018).
14. Meier, T., Khandarkhaeva, S., Jacobs, J., Dubrovinskaia, N. & Dubrovinsky, L. Improving resolution of solid state NMR in dense molecular hydrogen. *Appl. Phys. Lett.* **115**, 131903 (2019).
15. Meier, T. et al. In situ high-pressure nuclear magnetic resonance crystallography in one and two dimensions. *Matter Radiat. Extremes* **6**, 068402 (2021).
16. Meier, T. et al. Nuclear spin coupling crossover in dense molecular hydrogen. *Nat. Commun.* **11**, 6334 (2020).
17. Meier, T. et al. Structural independence of hydrogen-bond symmetrisation dynamics at extreme pressure conditions. *Nat. Commun.* **13**, 3042 (2022).
18. Yang, M., Zhou, Y., Jana, R., Nakagawa, T., Fu, Y. and Meier, T. Hexagonal to Monoclinic Phase Transition in Dense Hydrogen Phase III Detected by High-Pressure NMR. 1–6, 7 http://arxiv.org/abs/2407.19368 (2024).
19. Knight, W. D. Nuclear Magnetic Resonance Shift in Metals. *Phys. Rev.* **76**, 1259–1260 (1949).
20. Meier, T. et al. Pressure-Induced Hydrogen-Hydrogen Interaction in Metallic FeH Revealed by NMR. *Phys. Rev. X* **9**, 031008 (2019b).
21. Meier, T. et al. Proton mobility in metallic copper hydride from high-pressure nuclear magnetic resonance. *Phys. Rev. B* **102**, 1–8 (2020b).
22. Fu, Y. et al. Parts-per-billion trace element detection in anhydrous minerals by nano-scale NMR spectroscopy. *To Be Submitted*, 1–12, (2024).
23. Meier, T., Laniel, D. & Trybel, F. Direct hydrogen quantification in high-pressure metal hydrides. *Matter Radiat. Extremes* **8**, 018401 (2023).
24. Harris, R. K., Becker, E. D., Cabral de Menezes, S. M., Goodfellow, R. & Granger, P. NMR nomenclature: nuclear spin properties and conventions for chemical shifts. IUPAC Recommendations 2001. International Union of Pure and Applied Chemistry. Physical Chemistry Division. Commission on Molecular Structure and Spectroscopy. *Magn. Reson. Chem.* **40**, 489–505 (2002).
25. Man, P. P. Quadrupole Couplings in Nuclear Magnetic Resonance, General. In *Encyclopedia of Analytical Chemistry*, 12224–12265. John Wiley & Sons, Ltd, Chichester, UK, 9 (2006).
26. Klavins, P., Shelton, R. N., Barnes, R. G. & Beaudry, B. J. X-ray diffraction study of the cubic-to-tetragonal structural transformation in substoichiometric lanthanum trihydride and trideuteride. *Phys. Rev. B* **29**, 5349–5353 (1984).
27. Barnes, R. G., Beaudry, B. J., Creel, R. B., Torgeson, D. R. & de Groot, D. G. Electronic and structural transitions in stoichiometric and nearly-stoichiometric lanthanum trihydride and trideuteride. A 139La and 1H nuclear magnetic resonance study. *Solid State Commun.* **36**, 105–110 (1980).
28. Chen, D., Gao, W. and Jiang, Q. Distinguishing the structures of high-pressure hydrides with nuclear magnetic resonance spectroscopy. *J. Phys. Chem. Lett.* 9439–9445, (2020).
29. Laniel, D. et al. High-pressure synthesis of seven lanthanum hydrides with a significant variability of hydrogen content. *Nat. Commun.* **13**, 6987 (2022).
30. Errea, I. et al. Quantum crystal structure in the 250-kelvin superconducting lanthanum hydride. *Nature* **578**, 66–69 (2020).
31. Pake, G. E. Nuclear resonance absorption in hydrated crystals: Fine structure of the proton line. *J. Chem. Phys.* **16**, 327–336 (1948).
32. Slichter, C P*Principles of Magnetic Resonance*. Springer, Berlin, Heidelberg, second edition, (1978).
33. Levitt, M. Spin dynamics: Basics of nuclear magnetic resonance, 2nd edition. *Concepts Magn. Reson. Part A* **34A**, 60–61 (2009).
34. Hahn, E. L. Spin echoes. *Phys. Rev.* **80**, 580–594 (1950).
35. Bloembergen, N., Purcell, E. M. & Pound, R. V. Relaxation effects in nuclear magnetic resonance absorption. *Phys. Rev.* **73**, 679–712 (1948).
36. Hanabusa, M. & Bloembergen, N. Nuclear magnetic relaxation in liquid metals, alloys and salts. *J. Phys. Chem. Solids* **27**, 363–375 (1966).
37. Abragam, A and Hebel, L C*Principles of Nuclear Magnetism*, 18. Oxford University Press, Oxford New York, 18 edition, (1961).
38. Korringa, J. Nuclear magnetic relaxation and resonance line shift in metals. *Physica* **16**, 601–610 (1950).
39. Caussé, Maélie, Geneste, Grégory & Loubeyre, P. Superionicity of Hδ- in LaH10 superhydride. *Phys. Rev. B* **107**, 1–5 (2023).
40. Potzel, U., Raab, R., Völkl, J., Wipf, H., Magerl, A., Salomon, D. & Wortmann, G. Self-diffusion and collective diffusion of hydrogen in TaHx. *J. Less Common Met.* **101**, 343–362 (1984).
41. Žogal, O. J. & Cotts, R. M. Self-diffusion coefficient of hydrogen in NbH0.6. *Phys. Rev. B* **11**, 2443–2446 (1975).
42. Sakintuna, B., Lamari-Darkrim, F. & Hirscher, M. Metal hydride materials for solid hydrogen storage: A review. *Int. J. Hydrog. Energy* **32**, 1121–1140 (2007).
43. Labet, V., Gonzalez-Morelos, P., Hoffmann, R. and Ashcroft, N. W. A fresh look at dense hydrogen under pressure. I. An introduction to the problem, and an index probing equalization of H-H distances. *J. Chem. Phys.* **136**, 074501–074514 (2012).
44. Geballe, Z. M. et al. Synthesis and Stability of Lanthanum Superhydrides. *Angew. Chem. - Int. Ed.* **57**, 688–692 (2018).
45. Huot, J., Liang, G., Boily, S., Van Neste, A. & Schulz, R. Structural study and hydrogen sorption kinetics of ball-milled magnesium hydride. *J. Alloy. Compd.* **293-295**, 495–500 (1999).
46. Cross, S. et al. High-temperature superconductivity in La4H23 below 100 GPa. *Phys. Rev. B* **109**, L020503 (2024).
47. Buhot, J., Moulding, O., Muramatsu, T., Osmond, I. & Friedemann, S. Experimental evidence for orthorhombic Fddd crystal structure in elemental yttrium above 100 GPa. *Phys. Rev. B* **102**, 104508 (2020).
48. Osmond, I. et al. Clean-limit superconductivity in $Im\bar{3}m$ H_3S synthesized from sulfur and hydrogen donor ammonia borane. *Phys. Rev. B* **105**, L220502 (2022).
49. Majer, G., Renz, W., Seeger, A., Barnes, R. G., Shinar, J. & Skripov, A. V. Pulsed-field-gradient nuclear magnetic resonance studies of hydrogen diffusion in Laves-phase hydrides. *J. Alloy. Compd.* **231**, 220–225 (1995).
50. Wipf, H., Kappesser, B. & Werner, R. Hydrogen diffusion in titanium and zirconium hydrides. *J. Alloy. Compd.* **310**, 190–195 (2000).
51. Zheltikov, A. Understanding NMR Spectroscopy, James Keeler, John Wiley & Sons Ltd, Chichester, 2005, pp. 459, paperback, ISBN: 0470017872. *J. Raman Spectrosc.* **37**, 1456–1456 (2006).
52. Somayazulu, M. et al. Evidence for Superconductivity above 260 K in Lanthanum Superhydride at Megabar Pressures. *Phys. Rev. Lett.* **122**, 027001 (2019).
53. Kong, P. et al. Superconductivity up to 243 K in the yttrium-hydrogen system under high pressure - Supplement. *Nat. Commun.* **12**, 5075–5079 (2021).

Acknowledgements

We would like to acknowledge fruitful discussions with Ho-kwang Mao and Yang Ding. This work was supported by the National Key Research and Development Program of China (2022YFA1402301) and the National Science Foundation of China (42150101). T. Meier acknowledges financial support from Shanghai Key Laboratory Novel Extreme Condition Materials, China (no. 22dz2260800), Shanghai Science and Technology Committee, China (no. 22JC1410300). D.L. thanks the UKRI Future Leaders Fellowship (MR/V025724/1) for

financial support. I.O., O.M., J.B., and S.F. acknowledge support from EPSRC grants EP/V048759/1, EP/L015544/1 and ERC grant 715262-HPSuper. For the purpose of open access, the authors have applied a Creative Commons Attribution (CC BY) licence to any Author Accepted Manuscript version arising from this submission.

Author contributions

Idea and Conceptualization: T.M., Y.Z., M.Y.; Methodology: T.M. and Y.Z.; Investigation: M.Y., Y.Z, R.J., T.N., I.O.,D.L., S.F.,O.M., J.B., Y.F and T.M.; Visualization: Y.Z., and T.M.; Formal analysis: Y.Z., T.M.; Validation: M.Y., Y.Z., R.J., I.O., T.M., I.O., D.L., S.F., O.M., J.B.; Funding acquisition: T.M., S.F., D.L.; Resources: T.M., S.F., D.L.; Project administration: T.M.; Writing-original draft: Y.Z. and T.M.; Writing-review and editing: M.Y., Y.Z., R.J., T.N., Y.F, S.F., D.L., O.M., J.B., I.O. and T.M.

Competing interests

The authors declare no competing interests.

Additional information

Supplementary information The online version contains supplementary material available at https://doi.org/10.1038/s41467-025-56033-3.

Correspondence and requests for materials should be addressed to Thomas Meier.

Peer review information *Nature Communications* thanks the anonymous reviewers for their contribution to the peer review of this work. A peer review file is available.